Aspects of time-dependent deformation in hard rock at great depth

by K. Drescher* and M.F. Handley†

Synopsis

Excavations in deep level hard rock mines show rheological or time-dependent deformation responses to mining-induced stresses. These are generally not as dramatic as those seen in soft rock environments, such as potash and salt mines, but these deformations can nevertheless become substantial in time. It is usual to see total excavation closure at a much earlier stage than predicted by numerical models, and real-time measurements underground have confirmed that closure takes place on a more-or-less continuous basis, with highest closure rates observed after a blast and then slowly diminishing with passing time. This paper describes laboratory tests to determine the time-dependent response of hard rocks to loading, the results of the tests, and then quantifies these effects to explain the time-dependent phenomena observed underground. The primary intention of this work is to help explain the various time-dependent deformation processes around typical deep level hard rock tabular excavations. Three mechanisms were investigated in two typical hard rock types present in the deep level gold mines in South Africa, namely Ventersdorp Lava and Elsburg Quartzite. Uniaxial compression creep studies were done as the first part of the study followed by shear creep studies on discontinuities where crushed lava and crushed quartzite as well as a natural gouge were used as infilling. The last part of the study consisted of triaxial post-failure relaxation tests. The compression creep tests and the triaxial post-failure relaxation tests showed that the amount of energy dissipated by the lava is significantly less than for quartzite. For mines operating at depths greater than 2000 m the implication is that the lava must show a greater rockburst-proneness than the quartzite. Since the lava shows a lower post-failure stress relaxation, it can store sufficient energy for multiple rockbursts, which is seen in the clustering of multiple seismic events in the deep level mines. This study provides the first data available for energy change calculations in fractured rock masses, and provides the first general indications for rockburst intensities ahead of active mining faces.

Introduction

Closure measurements in South African hard rock mines show definite time-dependency or rheological properties[1], which are derived from at least four mechanisms: compression creep of the intact rock, rock material dilation arising from stress damage, shear creep on discontinuities, and discontinuity dilation with growing shear displacements. These mechanisms result in larger displacements (closures) than those predicted by elastic models, and to the eventual unravelling of the rock mass. Post-failure relaxation of the rock material may also play a role, although exactly how it would affect excavation closure is not clear. Mining excavation closure measurements can therefore be used to deduce rheological processes taking place in the rockmass surrounding the excavation[1,2]. This information is useful in determining optimum mining rates in different geotechnical environments[3]. Furthermore, the occurrence of rock bursts can be linked to the rheological response of hard rocks to mining-induced stress changes, so information on excavation deformation rates might one day be useful in predicting impending rockbursts.

Rheological rock properties are best known in softer, less brittle rock types such as rock salt and potash[4]. Significant creep is often observed in these rocks, even in shallow mines, where the overburden stress can often be close to the uniaxial compressive strength of the material. Creep in hard rock tends to be significantly less than in soft rock, which makes it that much more difficult to measure underground and in the laboratory. Until recently, rheological properties of hard rocks were almost completely ignored[2].

Data on uniaxial compression creep experiments are widely reported in the literature[5,6]. Nearly all studies investigated relatively soft, compliant rocks such as rock salt, potash, limestone, or shale. All these rocks can be regarded as relatively weak and soft in comparison to those found in deep South African hard rock mines, and show easily measurable creep behaviour. Amongst the stronger and stiffer rocks tested, there are many data for rocks such as shale with a uniaxial compressive strength of less than 50

* *CSIR Division of Mining Technology.*

† *Department of Mining Engineering, University of Pretoria.*

 SA ISSN 0038–223X/3.00 + 0.00. Paper received Jan. 2003; revised paper received Apr. 2003.

MPa, and sandstone (50-100 MPa)[2]. There are also data available on marble, which is a fairly stiff and strong rock (100-150 MPa)[2]. All these rock types are relatively compliant and plastic compared to Witwatersrand Quartzite (100 to 250 MPa) or Ventersdorp Lava (300 to 600 MPa), which are encountered in the deep rock burst-prone gold mines of South Africa. Most of the studies on uniaxial compression creep report only the strain-time data for the axial deformation and do not mention the lateral deformation[2].

In terms of creep testing of discontinuities, far less information is found in the literature[2]. Some triaxial compression experiments using cylindrical granite test specimens containing a discontinuity have been reported[7]. Amadei[8] proposed a hypothesis that the shear creep of a joint would be governed by the ratio of applied shear stress to peak shear strength. Schwartz and Kolluru[9] did some studies using a gypsum-plaster mix to test the hypothesis of Amadei[8]. Bowden and Curran[10] performed tests on artificial discontinuities prepared from shale. Malan[1] and Malan, Drescher, and Vogler[11] did more elaborate work on shear creep of discontinuities, which are commonly encountered in typical South African deep mines.

As far as the relaxation of failed rock is concerned, studies are limited to the relaxation of failed rock under uniaxial compression. Apart from Malan and Drescher[3], there is no evidence in the literature that triaxial post-failure relaxation studies have ever been carried out.

Mining-induced seismic events sometimes seem to be the result of rheological processes in the rock mass because they do not always occur immediately after the blast. Instead, many (about 50%) occur during the shift, many hours after the blast. The laboratory testing is intended to help quantify the various time-dependent deformation processes around typical excavations in South African deep level hard rock mines. Laboratory data on rheological properties will provide a basis for more detailed numerical modelling of highly stressed hard rock masses, improving understanding of time-dependent mechanisms that eventually result in mining-induced seismicity and rock bursts. This may eventually lead to a methodology to predict seismicity and rockbursts, which would provide a significant advance in the enhancement of safety in deep level hard rock mines.

This paper first describes the laboratory testing methods employed to determine the rheological properties of intact hard rock, discontinuities in hard rock, and post-failure relaxation in hard rock. The authors compare and contrast the results of the laboratory experiments, and attempt to quantify the effects of these phenomena in deep level mine excavations. The results should provide guidelines for future investigative modelling of rheological behaviour in hard rock masses at depth.

Laboratory experiments

The objectives of the laboratory testing programme were to determine the time-dependent behaviour of Elsburg Quartzite and Ventersdorp Lava (typical South African hard rocks) and then compare the results by:

- Obtaining more strain-time data (axial and lateral strain) under uniaxial compression by performing uniaxial creep studies on intact rock
- Gaining more insight into the time-dependent behaviour of discontinuities by performing direct shear creep tests using crushed rock as well as natural gouge as infilling
- Studying the axial stress relaxation of failed rock by performing triaxial post-failure relaxation studies.

Uniaxial creep experiments

The specimens were tested in the CSIR creep-testing machine, originally used by Bieniawski[12]. A computerized data acquisition system has replaced the original analogue system. The new system is fitted with an uninterruptible power supply unit. The machine is housed in a special climate controlled laboratory, where the temperature is kept constant at 20±0.5°C and the relative humidity is maintained at 50±2%. This is done to eliminate any effect temperature and moisture fluctuation might have on either the specimen or the equipment. The principle of operation is shown in Figure 1 and a typical experiment set-up is shown in Figure 2.

The test specimens were prepared in accordance with the ISRM[13] suggested methods for uniaxial compressive strength tests with deformability measurements. Axial and lateral strain measurements were obtained by means of strain gauges and additional axial strain measurements were done using LVDTs (Linear Voltage Differential Transformer). This was done to confirm the axial strain, because there is a

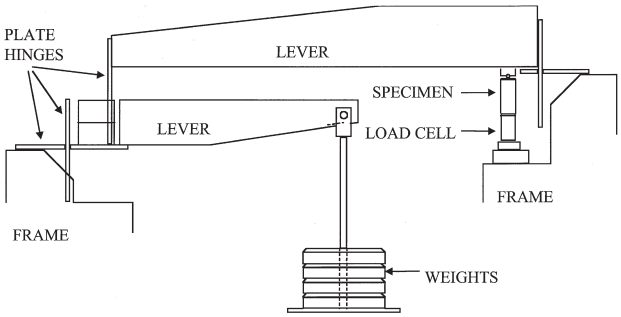

Figure 1—Principle of operation of the CSIR creep testing machine

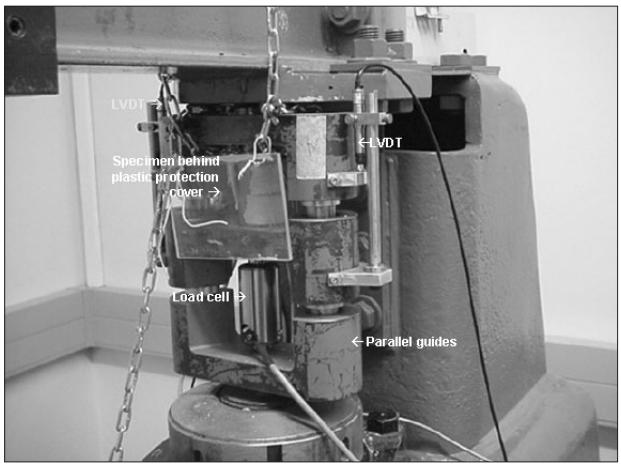

Figure 2—Typical experimental set-up for uniaxial creep tests in the laboratory

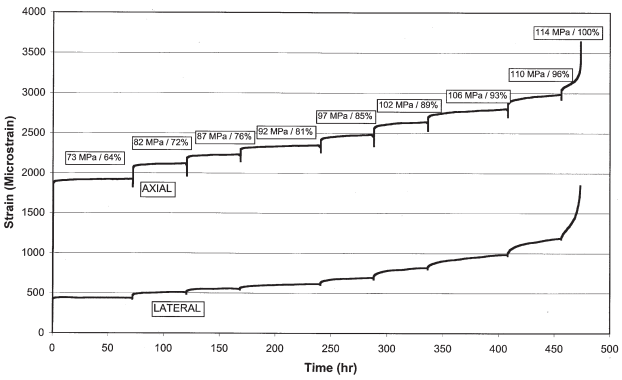

Figure 3—Result of a uniaxial compression creep test of hard rock

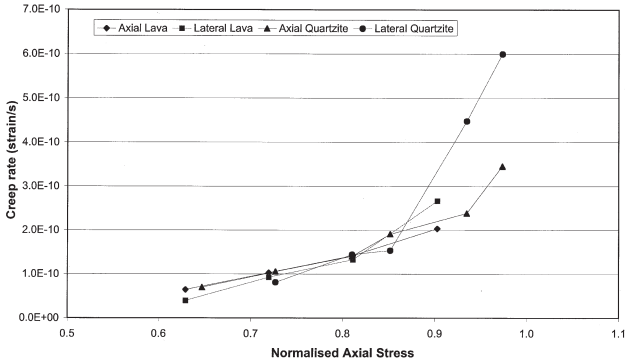

Figure 5—Plot of creep rate versus normalized axial stress for quartzite and lava

possibility that the strain gauges themselves could creep, masking the actual creep strain in the specimen. The accuracy of the strain measurements is within the ISRM[13] specifications, i.e. within 5 x 10^{-6} strain for the strain gauges and within 0.002 mm for the LVDTs. The axial load is maintained perfectly constant due to the deadweight loading arrangement, excepting when the load increment is increased.

The specimens were tested using a step-wise loading procedure during which the specimens were initially loaded to approximately 60% of the expected failure load. After a period of 48 hours, the load was increased by approximately 5%. The 48-hour period was chosen by trial and error, since it has been observed that there is usually no further significant creep in the specimen 48 hours after a loading increment. The 48-hour cycle of loading and waiting was repeated until specimen failure. A typical test result is shown in Figure 3.

Figure 4 shows the axial and lateral creep rates against axial stress for quartzite and lava. The Figure clearly shows that similar creep rates in lava and quartzite occur at significantly different stress levels. If the stresses are normalized (stress level divided by uniaxial rock strength) the curves for lava and quartzite are very similar as shown in Figure 5. It is worth noting in both cases that the lateral creep rate increases faster than the axial creep rate when the stress levels approach the strength of the material. This suggests that fracture and failure mechanisms in both rock types are similar despite differences in their geological origin (the lava is an igneous rock, the quartzite sedimentary), granular structures, and physical properties.

The test results are summarized in Table I. The 'nosepoint' is defined by Bieniawski[12] as the point of maximum volumetric strain or the onset of unstable fracture propagation. The parameters determined for the steady-state creep law as well as energy calculations are given in Table II.

The following observations were made from the laboratory data[2]:

- Very hard and brittle rocks, if subjected to sufficient stress, show creep behaviour
- For the lava, the 'nosepoint' occurs at a higher stress/strength ratio than for the quartzite
- For lava and quartzite, the amount of creep strain as well as the creep rate is proportional to the applied stress/strength ratio
- The ratio between the loading modulus and unloading modulus for the quartzite is significantly lower than for the lava indicating that the damage done to the quartzite specimens is greater than the damage done to the lava specimens
- The average creep strength for both the quartzite and the lava are lower than the respective uniaxial compressive strength
- Although the modulus values for the lava are higher than those of the quartzite specimens, the maximum strain at failure of the lava is higher than that of the quartzite

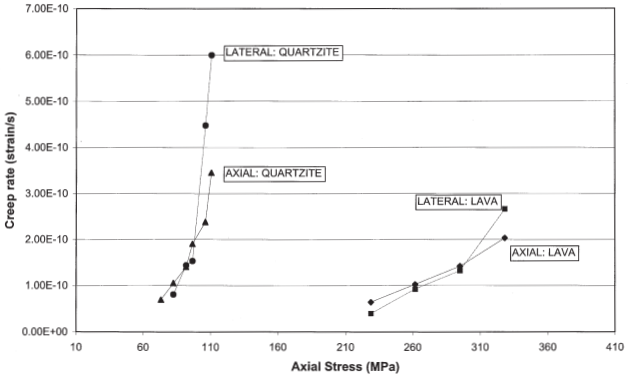

Figure 4—Plot of creep rate versus axial stress for quartzite and lava

Table I

Uniaxial compression creep results (after Drescher[2])

Specimen No	Creep Strength (MPa)	Nosepoint Stress (MPa)	Nosepoint as % Strength	Axial Strain at Failure x 10^{-6}	Modulus Loading (GPa)	Modulus Unloading (GPa)	Damage Index
Ventersdorp Lava							
1640-23	363.7	328.2	90.3	4645	84.7	96.8	0.88
1640-53	435.4	397.4	91.3	5135	92.8	101.2	0.92
1640-55	398.7	361.9	90.8	4039	93.8	109.5	0.86
1640-63	402.2	330.3	82.1	4582	89.1	101.8	0
Elsburg Quartzite							
2056-116	117.6	91.0	77.4	3055	39.5	76.5	0.52
2056-117	114.1	91.9	80.5	3642	40.7	75.2	0.54
2056-118	112.6	91.0	80.9	4142	39.7	73.9	0.54
2056-121	135.2	105.9	78.3	3267	51.0	79.7	0.64

Table II

Power law parameters and energy calculations (after Drescher[2])

Spec No	% Strength	Axial Creep rate (strain/s)	Lateral Creep rate (strain/s)	Axial 'n'	Axial log(A')	Lat. 'n'	Lateral log(A')	Energy Dissipation (kJ/m^3)	Total Energy at % Strength (kJ/m^3)	Percentage Energy Dissipation
Ventersdorp Lava										
1640-23	90	2.03E-10	2.67E-10	3.15	-36.5	5.06	-52.7	64.0	671.3	9.5
1640-53	91	3.14E-10	3.33E-10	4.24	-46.1	5.08	-53.3	91.8	922.7	10.0
1640-55	91	1.06E-10	1.44E-10	6.90	-68.6	5.33	-55.5	48.5	728.8	6.7
1640-63	91	3.36E-10	4.83E-10	7.96	-77.7	5.98	-60.6	102.3	799.8	12.8
Elsburg Quartzite										
2056-116	89	1.83E-10	2.75E-10	2.14	-27.0	4.06	-35.2	23.4	137.1	17.1
2056-117	93	2.39E-10	4.47E-10	3.70	-39.3	13.30	-108.7	27.1	147.8	18.4
2056-118	91	2.72E-10	3.53E-10	5.76	-55.5	10.55	-86.6	26.0	143.3	18.1
2056-121	93	4.69E-10	9.83E-10	4.40	-45.1	6.30	-53.0	29.0	163.9	17.7

- The percentage energy dissipation for the quartzite is significantly higher than for the lava, showing that the quartzite is relatively more 'plastic' than the lava
- There is three times more strain energy stored in the lava than in the quartzite at failure.

The potential for violent rockbursts is therefore far greater in the lava than in the quartzite.

Shear creep on discontinuities

The tests were performed using the shear-creep apparatus as described by Vogler, Malan and Drescher[14], and shown in Figure 6. Artificial joint surfaces were used for these tests, since the object of the experiments was to study creep in the discontinuity infillings. Three infillings were used: (1) crushed lava, (2) crushed quartzite and (3) natural gouge collected at Hartebeestfontein Mine. All three infillings were sieved to a size smaller than 500 microns, and particle size distribution analyses were done for all three infilling materials, which showed the following[2]:

- The crushed quartzite consists mainly (±30%) of material with a particle size of between 20 and 40 microns as well as between 200 and 500 microns
- The crushed lava consists mainly (±60%) of material with a particle size of between 300 and 600 microns
- The natural gouge consists mainly (±80%) of material with a particle size of between 10 and 40 microns.

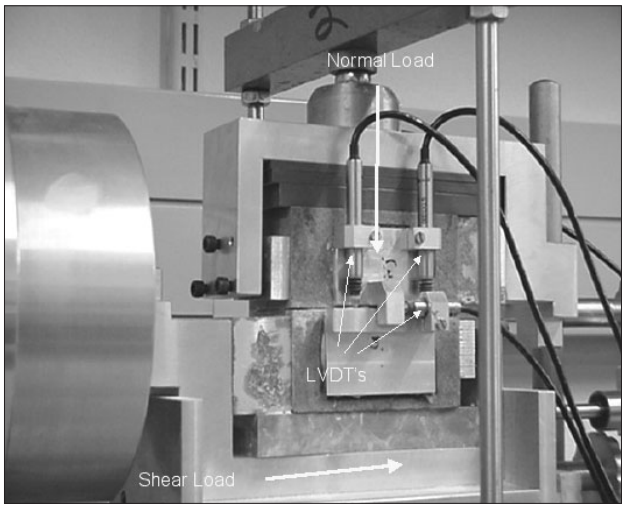

Figure 6—Shear creep apparatus

Although all three materials were sieved with a 500-micron sieve, the particle size distribution shows material between 500 and 1000 micron for the quartzite and the lava, which indicates that some of the particles were elongated. Comminution should have a significant effect on the creep properties of the infill materials, but available equipment does not have the capacity to investigate its effects.

The creep testing machines are housed in the same climatically controlled laboratory as the compression creep testing machine, with a temperature of 20±0.5°C, and a relative humidity of 50±2%. Under these conditions, the displacement measurements are accurate to 0.002 mm. At a typical air pressure of 54 kPa, the pressure and thus the shear load remains constant within 0.25%. These accuracies exceed the relevant ISRM[15] specification for shear testing. The normal force remains constant due to the deadweight arrangement

Three infilling thicknesses were studied, 0.5 mm, 1 mm, and 2 mm. Two humidity conditions were used, the first 50% humidity, and the second, 100% humidity, which implies mixing the infilling with water and keeping it saturated during testing. Similar to the compression creep a step-wise loading procedure was followed, with time intervals of 48 hours.

A maximum of 1.5 MPa normal stress can be applied to the specimen in the creep testing machines, because of its design and structure. Although this is far lower than the normal stresses expected to act across discontinuities in hard rock at depth, the shear creep tests are nevertheless expected to provide insights into shear creep behaviour, even at these stress levels. Since a vertical stress of 1.5 MPa would place a severe strain on the machine, all the shear creep tests were carried out at 0.65 MPa normal stress[2]. This low normal stress will not result in further comminution of the infill material as the discontinuity creeps, which is expected to happen on discontinuities in highly stressed rock masses. Comminution of infill material is expected to have the effect of lowering the shear strength of discontinuities, and should be the subject of further laboratory studies in the future.

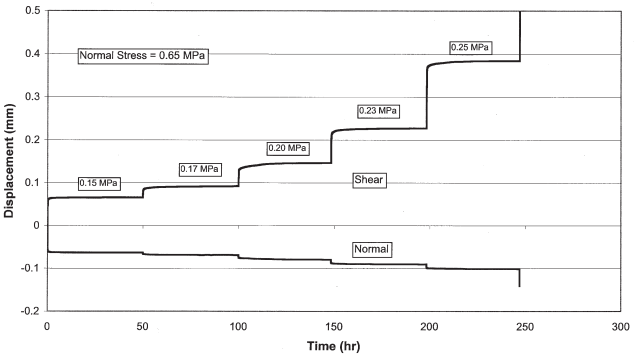

Figure 7—Typical shear displacement versus time curve for shear loading on a discontinuity (after Drescher[2])

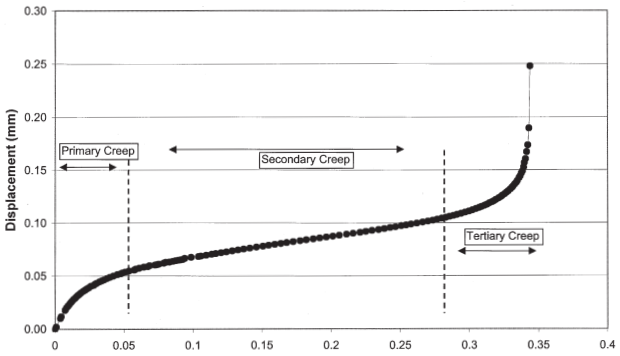

Figure 8—Classical creep behaviour of a discontinuity in shear (after Drescher[2])

A typical test result is shown in Figure 7. It is clear in the Figure that the primary creep step sizes increase with each new load increment, and the steady state (secondary) creep rate increases with each subsequent loading increment. The shear creep results thus display similar characteristics to the compression creep results, namely that the primary creep increases with the shear stress to shear strength ratio, and that the secondary creep rate also is related to the shear stress to shear strength ratio. Figure 8 shows a test result that displays all three classical creep phases seen in compressive creep tests; only in this case it is a shear creep test. As with compressive creep tests, shear creep follows the classical creep phases, namely primary, secondary, and tertiary creep just prior to failure. This confirms that the three phases of creep, usually only associated with compression creep, also exist when a discontinuity is subjected to shear loading. As far as the authors know, no such curve for shear creep has ever been produced in the laboratory before. The classical compression creep law is thus also applicable to shear creep on filled discontinuities in rock.

The test results are summarized in Table III. The following observations were made.

- At the same applied normal stress the peak shear strength of the discontinuity filled with natural gouge is much lower than those filled with crushed quartzite or crushed lava.
- Primary, secondary and tertiary creep phases were observed.
- The creep rate is dependent on the shear stress to shear strength ratio: a higher ratio leads to a higher creep rate as well as to a larger displacement in a given time period.
- The creep rate is significantly influenced by the moisture content: more moisture leads to higher creep rates as well as larger displacements in a given time period.
- The ratio of grain size to infilling thickness as well as the grain size distribution have a significant influence on creep behaviour at low normal stresses, although this is expected to diminish with increasing normal stress (see first observation above for natural gouge).

Table III

Summary of shear creep test results (after Drescher[2])

Spec.No	Thickness (mm)	τ/τ_s(%)	Humidity (%)	Peak Friction angle (°)	Shear Creep rate(mm/hr)	n	Log A	Shear Energy Dissipation (kJ/m^2)	Total Shear Energy at τ/τ_s (kJ/m^2)	Percentage Shear Energy Dissipation
Crushed Elsburg Quartzite										
2056-143	0.5	92	50	19.5	1.53E-04	4.46	-10.19	0.0036	0.0076	47.4
2056-144	1	90	50	29.6	1.50E-04	3.54	-10.32	0.0180	0.0250	71.7
2056-145	2	91	50	28.2	1.60E-04	2.54	-10.27	0.0160	0.0410	37.7
2056-146	1	89	100	28.5	4.42E-04	3.78	-9.82	0.0340	0.0430	81.1
Crushed Ventersdorp Lava										
2056-162	0.5	92	50	23.1	1.21E-04	2.89	-10.35	0.0190	0.0490	37.9
2056-148	1	90	50	30.5	6.15E-05	5.33	-10.41	0.0190	0.0380	55.2
2056-149	2	89	50	30.7	4.60E-05	3.82	-10.7	0.0160	0.0290	55.2
2056-150	1	90	100	31.9	2.86E-04	3.58	-9.97	0.0330	0.0500	66.6
Natural Gouge										
2056-239	0.5	94	50	17.5	2.41E-05	0.38*	-11.64*	0.0028	0.0056	50.0
2056-238	1	91	50	20.3	5.69E-05	1.84	-10.66	0.0086	0.0160	54.6
2056-240	2	89	50	20.8	5.81E-05	7.24	-10.44	0.0140	0.0210	67.5
2056-241	1	89	100	18.5	8.75E-05	3.89	-10.47	0.0140	0.0190	72.8

* Only two data points

- The effect of infill particle comminution due to discontinuity sliding is probably not significant in these experiments, but it will have the effect of lowering the shear strength of the discontinuity, and perhaps accelerating the onset of tertiary creep (see first observation above for natural gouge).

When studying Table III it is noteworthy that for the crushed quartzite and crushed lava, contrary to the natural gouge, the values for peak friction angle at a thickness of 0.5 mm is much lower than those at a thickness of 1 mm and 2 mm respectively. As the particle size of 500 microns (0.5 mm) is very close to the thickness of the infilling, it appears that the mechanism of displacement for discontinuities with 0.5 mm thick infilling may differ to those in tests where the thickness of the infilling is significantly larger than the particle size. If the normal force is not high enough to crush the individual grains, two types of shear creep mechanism are proposed.

Single layer mechanism (rolling of grains)

In this mechanism, there is one layer of grains between the two sides of the discontinuity, which would just roll over each other. An analogy to this mechanism is a ball bearing or a roller bearing, especially when the sides of the discontinuity are without any asperities. The grains act similarly to the steel rollers in a roller bearing. This mechanism could explain the lower friction angles for the quartzite and lava discontinuities at a thickness of 0.5 mm. Since the major particle size for the natural gouge is much smaller, this mechanism is not applicable to the natural gouge if the infilling thickness is 0.5 mm.

Composite layer mechanism

For this mechanism, considerable compaction of the material occurs during any relative movement of the two sides of the discontinuity. The material would be packed tighter increasing the friction between the grains, which would lead to an overall greater resistance and bigger friction angle values. Since there is probably no grain crushing involved, the crushed quartzite and lava infillings show different characteristics to the natural gouge. The authors expect the three infillings to behave more similarly in cases where the normal stress on the discontinuity is sufficiently high to result in infill particle crushing.

The shear creep tests have produced some significant results, but it must be borne in mind that the effect of infill particle comminution is probably absent, and that this will contribute to lowering the ultimate shear strength of discontinuities in highly stressed hard rock masses. Therefore, laboratory experiments with normal stresses on hard rock discontinuities approaching those observed in deep level mines are necessary before any generic conclusions can be drawn for shear creep in hard rock.

Post-failure relaxation

As far as the authors know, nobody has been able to conduct post-failure relaxation tests on strong brittle rocks successfully until the tests reported by Malan and Drescher[3]. Post-failure relaxation tests have been reported for softer rocks in the literature, for example Hudson and Brown[16], who tested Cherokee Marble with a uniaxial compressive strength of 55 to 62 MPa. Cherokee Marble is both much weaker and more plastic than the quartzite and lava discussed here, but it is the strongest rock for which post-failure relaxation tests have been reported in the literature[2].

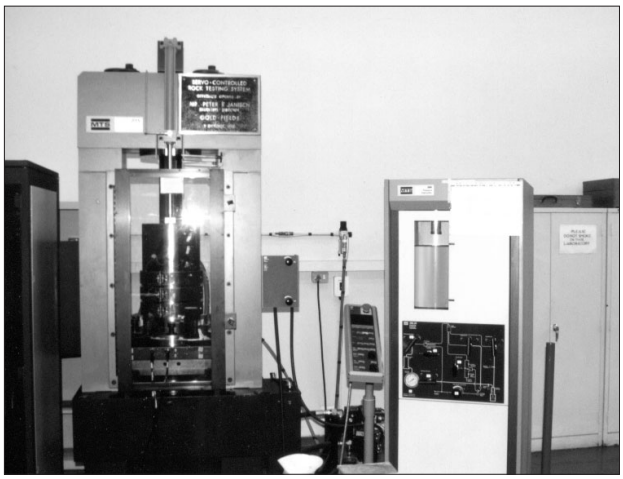

Figure 9—MTS testing machine

The experiments of Malan and Drescher[3] and the experiments reported in this paper were undertaken on an MTS Model 850 uniaxial and triaxial rock-testing machine at the University of the Witwatersrand, Johannesburg. The machine is shown in Figure 9. The triaxial tests were carried out with a lateral confinement of 40 MPa, and when the predetermined post-failure load-level is reached, the machine is switched to the 'relaxation' control mode, during which the axial ram position as well as the confinement are kept constant for 24 hours, which time span was chosen as described below. The load, time and circumferential strain data is logged during the test. The accuracy of the strain measurement transducers of the MTS machine is in accordance with the ASTM[17] testing methods. Over the relaxation period of 24 hours the machine piston was maintained in a fixed position within 0.0005 mm and the confinement of 40 MPa was maintained to within 0.005 MPa.

When Hudson and Brown[16] undertook their post-failure relaxation tests on Cherokee Marble, they used relaxation periods of 600 seconds (10 minutes). The relaxation curves

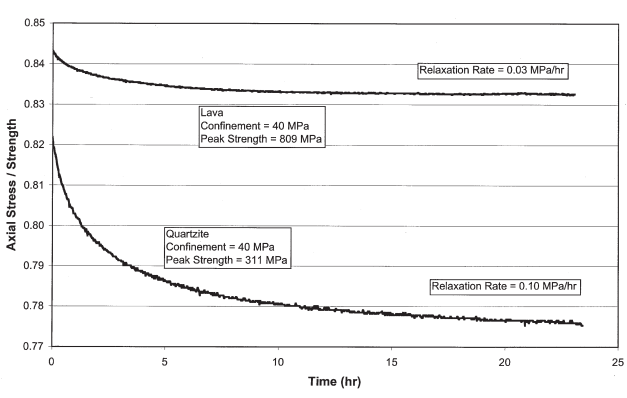

Figure 10—Post-failure relaxation curves for quartzite and lava

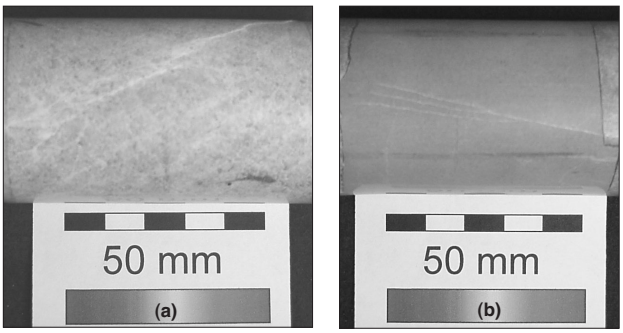

Figure 11—Fracture damage to (a) quartzite and (b) lava

they obtained display an exponential decay, flattening to constant values within the 600-second period. It was expected that harder rock confined at 40 MPa would have a longer relaxation time, thus a hold time of 2 hours was applied initially. This proved to be not nearly long enough and the relaxation time period was increased to 24 hours, which was found to be sufficiently long to include the complete stress relaxation profiles for hard rocks.

Relaxation curves for lava and quartzite are shown in Figure 10. The amount of stress relaxation in the quartzite is significantly more than in the lava. Figure 11 shows the tested specimens and it is very apparent that the quartzite shows a well-developed fracture pattern while the lava only shows a few cracks. The test results are summarized in Table IV. A number of attempts to start the relaxation period for the lava at a higher post-failure stress/strength ratio were unsuccessful—the specimens would be stable for one to two hours and then fail violently. This characteristic of lava is responsible for face bursts in mines exploiting the Ventersdorp Contact Reef, and will be discussed in more detail later.

The most important findings for the post-failure relaxation tests are as follows.

- Under a fairly high confinement the post-failure relaxation periods for quartzite and lava are approximately two orders of magnitude larger than the relaxation periods required for Cherokee Marble under uniaxial post-failure conditions.
- The more coarse-grained quartzite specimens show a well-developed fracture pattern after testing, while the extremely fine-grained lava specimens only show a few cracks.
- At a confinement of 40 MPa, the triaxial peak strength of lava is more than twice that of the quartzite.
- At similar stress to strength ratios in the post-failure region, quartzite shows significantly more stress relaxation than lava for a given time period.
- The stress relaxation rate is higher for the quartzite than the lava.
- During the relaxation process the axial deformation is kept constant which means that the energy dissipation is expressed in the circumferential strain during relaxation.
- The total strain energy in the specimen before relaxation is significantly greater in the lava than in the quartzite.
- At similar stress to strength post-failure ratios, the percentage specific energy dissipation for the lava is much lower than for the quartzite.

Discussion of experimental results and their significance underground

Malan[1] describes the difficulties in applying viscoelastic and viscoplastic analytical models to stope closure profiles measured underground. He concludes that these models are continuum models, which cannot take the effects of rock fracture and creep on rock discontinuities into account. Numerical modelling produces somewhat better results[1], but again failed to reproduce the closure measurements satisfactorily, because the analyses were limited in scope, and the results were path-dependent. Thus, Malan[1] did not quantify the relative importance of the various mechanisms that are responsible for rheological hard rock deformation around deep mine openings, although insights from his work suggest that compression creep is an insignificant contributor to time-dependent stope closure.

During the triaxial post-failure relaxation tests, it was noted that the specimens appear to be very unstable in the post-failure region if the post-failure stress level is close to the failure strength. This is particularly true of the lava,

Table IV

Summary of post-failure relaxation tests (after Drescher[2])

Specimen No	Peak Strength (MPa)	σ/σ_c starting point	Relaxation rate (MPa/hr)	Circumferential strain rate (microstrain/hr)	Energy dissipation (kJ/m^3)	Energy at start of relaxation (kJ/m^3)	Percentage Energy dissipation
Elsburg Quartzite							
2056-105	324	0.56	0.14	6.7	25.0	1938	1.29
2056-106	479	0.74	0.11	2.6	26.9	1983	1.36
2056-157-1	311	0.82	0.10	6.6	15.2	1704	0.89
2056-157-2	311	0.72	0.09	3.8	13.1	1689	0.77
2056-157-3	311	0.62	0.05	1.3	3.9	1676	0.23
Ventersdorp Lava							
2056-123	809	0.84	0.03	8.2	12.8	3834	0.33

which will sustain such high stress levels for a few hours, and then fail violently. Observations suggest that instability of the test specimens is related to their strength and their brittleness. A stronger, more brittle rock (in this case the Ventersdorp Lava) exhibits more catastrophic loss of strength as a result of a relatively lower level of damage than does a more ductile specimen (in this case the quartzite), as is shown in Figure 11. Relatively less strain energy is absorbed in material damage in lava than in quartzite, while relatively more strain energy is stored by the lava because of its greater strength. Thus,more strain energy is available for sudden release in violent failure in the lava than in the quartzite. Creep itself is not a driving mechanism of failure, it is merely an outwardly measurable manifestation of failure processes taking place in a stressed material. Thus, creep is a measure of the complex interaction between loading of a material, the material damage developing within by whatever mechanism, and the slow resulting reduction of the stress:strength ratio towards unity, where creep rates increase dramatically and failure occurs. Mechanistically, creep is a physical measure of a material's ability to:

- dissipate strain energy in material damage, and therefore is a rough measure of the potential violence of material failure
- withstand the current loading for a given amount of time.

As stated in the introduction, there are at least four mechanisms responsible for time-dependent hard rock deformation, namely:

- compression creep of the intact rock material
- material dilation as a result of stress damage
- shear creep on pre-existing discontinuities and stress-induced discontinuities in the rock
- dilation of discontinuities as shear displacements grow with time.

The latter two are distortion-type mechanisms, which combine to produce nearly all the time-dependent closure seen in deep excavations, while the former two volumetric-type mechanisms contribute very little. This is in contrast to the softer rocks such as rock salt, which show much larger volumetric deformation components. It is possible that lateral dilation in hard rock will cause visible bulging in a deep stope face, although no known measurements of this phenomenon have ever been made. In what follows, the authors estimate the amount of compression creep that typically would occur in hard rock 3000 m below surface, and then relate this to the observed closure rates seen in deep stopes.

Consider the rockmass ahead of a deep longwall in hard rock, which experiences a concentration of compressive stresses ahead of the mine face, and decompression behind the mine face. The situation is illustrated in Figure 12 based on an elastic analysis by Wagner[19], who contoured the major principal stress concentration factors above, below, and in front of a horizontal stope in an elastic medium. Wagner did not consider the direction of the major principal stress component, merely contouring the stress concentration factors, which can be applied to a stope at any depth. Consider the rock ahead of the face as an imaginary vertical column, which is subjected to different stress concentrations along its length. The imaginary column is drawn to the right of Wagner's[19] stress diagram for clarity, and the stress concentration factors are listed within the column.

To simplify the calculations, we assume the following.

- The major principal stress component is vertical throughout the length of the column, the only change being the magnitude of the stress concentration factor with depth in the column.
- The minor principal stress is always horizontal, and equal to half the major virgin principal stress throughout the column, i.e. the stoping does not influence the horizontal stress significantly (this assumption may err toward exaggerating creep displacements, since there is some horizontal stress concentration ahead of the face, which could reduce vertical creep).
- The major virgin principal stress is vertical, and equal to the overburden weight, and for this calculation is assumed to be 80 MPa, corresponding to a stope approximately 3000 m below surface.
- The compression creep process is independent of confinement (this is generally not true).
- The compression creep process arises from a combination of intact rock material creep and stress-induced material damage, as is observed in the laboratory.

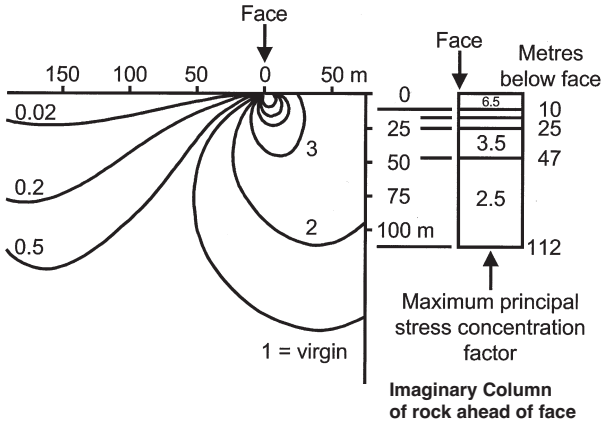

Figure 12—Maximum principal stress concentration ahead of a deep longwall

Table V

Compression creep rate estimations from linear regression

Vertical Distance from Stope (m)	Stress Concentration Factor	Stress Difference ($\sigma_1 - \sigma_3$) (MPa)	Stress to Strength Ratio - Lava	Creep Rate – Lava (s^{-1})	Stress to Strength Ratio - Quartzite	Creep Rate – Quartzite (s^{-1})
0 –10	6.5	480	0.75	1.25e-10	1.33	5.27e-10
10 – 18	5.5	400	0.63	0.39e-10	1.11	3.74e-10
18 – 25	4.5	320	0.50	0.00	0.89	2.21e-10
25 – 47	3.5	240	0.38	0.00	0.67	0.67e-10
47 – 112	2.5	160	0.25	0.00	0.44	0.00

Notes:

1. The Least Squares Creep Rate Regression Line is given by

$$\dot{\varepsilon}_c = (-39.26 + 68.98\frac{stress}{strength})x10^{-11}\ s^{-1}$$ with a correlation coefficient r = 0.94.

2. Lava Creep Strength for Column = 400 + 6x40 = 640 MPa.
3. Quartzite Creep Strength for Column = 120 + 6x40 = 360 MPa.

Table VI

Daily creep displacements in column

Vertical Distance from Stope (m)	Daily Creep in Lava Column (mm/day)	Daily Creep in Quartzite Column (mm/day)
0 – 10	0.11	0.46
10 – 18	0.03	0.26
18 – 25	0.00	0.13
25 – 47	0.00	0.13
47 - 112	0.00	0.00
Total	0.14	0.98

- Rock strength is linearly related to confinement by *Rock strength* = $\sigma_c + 6\sigma_3$[16].
- σ_c is the average uniaxial creep strength for the lava and quartzite obtained from Table I.
- The creep rate is linearly related to the vertical stress to rock strength ratio, and the creep rate can be found from the axial creep rate measured in the compression creep experiments described in an earlier section and plotted in Figure 5.
- The linear relationship between stress to rock strength ratio and axial creep rate is based on a least squares best fit line to the data in Figure 5, and is identical for the lava and the quartzite (i.e. both quartzite and lava data are used to find the least squares line).

The calculations appear in Tables V and VI. The reason for choosing a whole column is to demonstrate that creep displacements in hard rocks remain small, even when including large volumes of rock in the calculations (in this case a column extending 112 m above or below the stope). The total daily shortening of a 224-metre column composed of lava in the hangingwall and quartzite in the footwall due to compression creep is estimated from the calculations described to be 1.12 mm. For a similar column of quartzite throughout, the estimated daily shortening due to compression creep is 1.96 mm. These figures are for the column as a whole. Stope closure due to compression creep is much smaller, and for a one metre stoping width in quartzite, it is estimated at 0.05 mm daily, and for a face in lava, 0.01 mm daily. These are very insignificant amounts when compared with 20–40 mm/day closure rates in deep Carbon Leader Reef stopes, and 10–30 mm/day closure rates in deep Ventersdorp Contact Reef stopes.

Compression creep can therefore be neglected as a mechanism responsible for time-dependent closure of mining excavations in hard rock. Unless there is another unknown mechanism, time-dependent stope closure in deep hard-rock mines must be almost exclusively caused by creep on discontinuities and the resulting dilation of these discontinuities. Malan[1] and Drescher[2] have already shown that significant creep can take place on discontinuities in hard rock, but this work is incomplete, as it has only covered infilled discontinuities with low confining stress. Malan[1] also reports that there is no creep on unfilled discontinuities at the low confinement levels presently possible. This is to be expected because there will be no rock material comminution on the discontinuity interfaces, and relative displacements other than sliding will not take place. At high confinements, the picture is expected to be different. Therefore, this work should be extended to stress-induced discontinuities, and natural discontinuities with and without infilling with high confining stress.

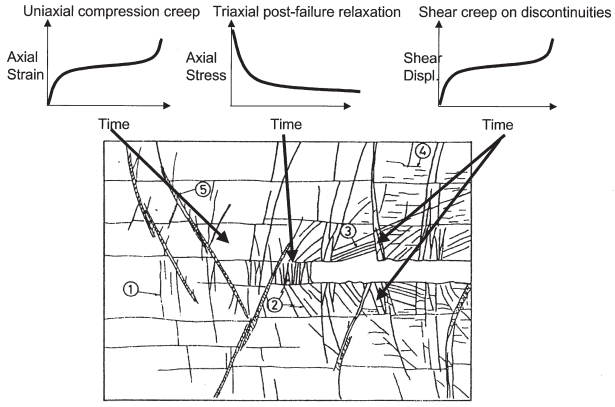

Figure 13—Stope fracture model after Gay and Jager[18] showing relevance of laboratory experimental results to time-dependent processes

The laboratory results can be related to the underground situation using a stope fracture model, first described by Gay and Jager[18], and shown in Figure 13. Both the violent and non-violent rock mass responses to mining at great depth are represented by the laboratory experiments described above. The compression creep deformation of the intact rock ahead of the face can be estimated from the results of the uniaxial compression creep tests, as has been demonstrated above. The stress-relaxation of the failed rock just ahead of the face results in some creep displacement, since in the mining situation there will be a following load caused by the weight of the overlying strata. The stress-relaxation rate may play an important role in the mining rate because if the mining rate is faster than the relaxation rate of the failed rock the stress just ahead of the face will increase, leading to an increased possibility of a face burst.

Handley[21] described such events at Western Deep Levels Mponeng Mine in which it was clear that the lava in the face of an off-reef stope is loaded by mining-induced stresses to approximately 90% of its strength (350 MPa) and then fails explosively after several hours, often during the face shift the next day. Such events are highly hazardous because they come without warning, and they seldom occur immediately after the blast, when nobody is in the stope.

The time-dependent shear displacement on discontinuities surrounding the stope appears to be the major mechanism driving time-dependent stope closure. Until measurements of this phenomenon are available, rock engineers can only model and speculate on its effects. Handley *et al.*[22] developed a borehole dislocation sensor that could be used to measure shear creep on discontinuities underground. The instrument was designed, manufactured, and tested on surface, but it was never installed underground. This work provides a good opportunity to measure shear creep on discontinuities *in situ*. Current shear creep tests demonstrate the creep characteristics of infilled discontinuities in hard rock at low confining stress (<1.5 MPa), and are therefore not considered relevant to filled and unfilled discontinuities in a highly stressed rock mass.

Malan[1] has demonstrated the effect of fault creep on a deep level stope in a numerical model, where the total fault creep of 3.1 mm generated in the analysis will probably be expressed as stope closure. This, however, is modelling

without supporting physical measurement. He also obtained a reasonable correspondence between measured closures and the results of a continuum elasto-viscoplastic numerical model for a small-span tabular excavation. Unfortunately, this is a continuum model, and cannot be used to estimate the effects of discontinuity creep on stope closure.

Conclusions

Typical South African hard rocks were subjected to uniaxial and triaxial compression and their time-dependent response was measured. Creep parametres suitable for use in numerical investigations have been determined from the measurements for hard rocks. This, in itself, is an achievement, because it has not been done successfully before. It has been shown that if hard rocks are subjected to sufficient uniaxial compressive stress they do exhibit well-defined time-dependent behaviour, albeit on a far smaller scale than for soft rocks. Significantly, quartzite and lava show similar axial and lateral creep rates at similar stress to strength ratios. It is, furthermore, noteworthy that although the strength of lava is more than twice as high as that of the quartzite the strain at failure of the lava is more than that of the quartzite. It is also evident from the results that the onset of unstable fracture propagation for lava occurs at a higher stress to strength ratio than for the quartzite. When measuring the deformation modulus during loading and unloading, quartzite shows more material damage than the lava.

For a discontinuity that contains an infilling and is subjected to a normal stress, the application of a constant shear stress will lead to shear deformations that exhibit primary, secondary and tertiary creep phases. It was also determined that higher shear stress to discontinuity strength ratios lead to higher shear creep rates. Furthermore, it is evident that for all three joint infill materials, the moisture content has an influence on the amount of time-dependent shear displacement as well as the shear creep rate. More experiments are needed to determine this exactly. The test results show that the shear creep mechanism is governed by the ratio between the thickness of the infilling and the grain size distribution of the infilling.

Triaxial post-failure relaxation tests were done using a confinement of 40 MPa. The first conclusion is that the post-failure relaxation time periods for hard rocks under a high confinement are orders of magnitude greater than the relaxation periods for softer rocks under uniaxial compression conditions. For mines, operating at great depth (more than 2000 m) the implication is that the rock material might relax much more slowly than might have been assumed and this means that after failure the rock mass continues to store large amounts of strain energy, which could again be released violently at a later date. This helps to explain the phenomenon of multiple seismic events coming from the same small volume in the rock mass.

Energy calculations for the compression creep tests show that for lava ±10% of the total applied energy is dissipated during the creep cycles while for quartzite ±18% of the total applied energy is dissipated. The total energy in the lava just before failure is three times as much as for the quartzite, indicating that in lava there is more energy available for violent failure than in quartzite. Hence, rockbursts in lava are perceived to be more violent than rockbursts in quartzite. Not only this, but more frequent as well, since The Chamber of Mines Research Organisation[20] records that rockbursts on the Ventersdorp Contact Reef are nearly four times as common for the same energy release rate than for the Carbon Leader Reef.

During shear creep tests on discontinuities with infilling, the energy dissipation for dry infilling varies between ±40% and ±70% for the different infilling materials. For saturated infilling the energy dissipation for the different infilling materials varies between ±65% and ±80%. For all three infilling materials the energy dissipation is more when the infilling is saturated.

During triaxial post-failure relaxation tests, at a stress to strength ratio of ±80% the energy dissipation for quartzite is ±0.90% compared to the lava where it is ±0.3%. Energy calculations show that for similar stress to strength ratios (post-failure) the percentage energy dissipation is significantly more for the quartzite than for the lava. Comparing the behaviour of quartzite and lava, the test results show that during a relaxation period of 24 hours the total stress relaxation for the failed quartzite is approximately twice that of the failed lava. The relaxation rate in the secondary relaxation phase for the quartzite is more than three times higher than for the lava.

Compression creep is an insignificant contributor to time-dependent excavation closure in deep level hard rock mines, while shear creep on discontinuities combined with discontinuity dilation are major contributors unless there are as-yet undiscovered deformation mechanisms. The authors believe that a full understanding of rock mass deformation and failure surrounding deep excavations in hard rock is close at hand. A full understanding will be reached by a combination of laboratory experiments on highly confined discontinuities, and *in situ* creep measurements on faults, joints and mining-induced discontinuities.

Acknowledgements

The authors wish to thank the CSIR Division of Mining Technology for their support, and permission to publish this paper.

References

1. Malan, D.F. An investigation into the identification and modelling of time-dependent behaviour of deep level excavations in hard rock. Ph.D. thesis, University of the Witwatersrand, Johannesburg, 1998.
2. Drescher, K. An Investigation into the Mechanisms of Time-Dependent Deformation of Hard Rocks. M.Sc. Dissertation, University of Pretoria, November 2002.
3. Malan, D.F. and Drescher, K. Modelling the post-failure relaxation behaviour of hard rock. In: *Proc. of the fourth North American Rock Mechanics Symposium,* edited by J. Girard, M. Liebman, C. Breeds, and T. Doe, Balkema, Rotterdam, 2000, pp. 909–917.
4. Latjai, E.Z., and Duncan, E.J.S. The mechanism of deformation and fracture in potash rock. *Can. Geotech. J.,* 25, 1988, pp. 262–278.
5. Price, N.J. A Study of the time-strain behaviour of coal-measure rocks. *Int. J. Rock Mech. Mining Sci.,* Pergamon Press, 1, 1964, pp. 277–303.
6. Singh, D.P. A study of creep of rocks. *Int. J. Rock Mech. Min. Sci. & Geomech.* Abstr., 12, 1975, pp. 271–276.
7. Wawersik, W.R. Time-dependent behaviour of rock in compression. In *Proceedings of the Third Int. Soc. Rock Mech. Congress,* Denver, 1974, pp. 357–363.

8. AMADEI, B. Creep behaviour of rock joints. M.Sc. thesis, University of Toronto, Canada, 1979.

9. SCHWARTZ, C.W. and KOLLURU, S. The influence of stress level on the creep of unfilled rock joints. In: *Proc. 25th Symp. Rock Mech.* edited by C. H. Dowding and M.M. Singh, 1984, pp. 333–340.

10. BOSMAN, J.D., MALAN, D.F., and DRESCHER, K. Time-dependent tunnel deformation at Hartebeestfontein Mine. *Proceedings of the AITES-ITA 2000 World Tunnel Congress,* SAIMM, Durban, 2000, pp.55-62.

11. MALAN, D.F., DRESCHER, K. and VOGLER, U.W. Shear creep of discontinuities in hard rock surrounding deep excavations. In: *Proc. Mechanics of faulted and jointed rock, MJFR-3*, edited by H.P. Rossmanith, Balkema, Rotterdam, 1998, pp. 473–478.

12. BENIAWSKI, Z.T. Mechanism of brittle fracture of rock. *Int. J. Rock Mech. Mining Sci.,* Pergamon Press, 4, 1967, pp. 425–430.

13. ISRM, Commission on Standardisation of Laboratory and Field Tests. Suggested methods for determining the uniaxial compressive strength and deformability of rock materials. *Int. J. Rock Mech. Min. Sci. & Geomech.* Abstr. vol. 16, 1979, pp. 135–140.

14. VOGLER, U.W., MALAN, D.F., and DRESCHER, K. Development of shear testing equipment to investigate the creep of discontinuities in hard rock. In *Proc. Mechanics of faulted and jointed rock, MJFR-3* edited by H.P. Rossmanith, Balkema, Rotterdam, 1998, pp. 229–234.

15. ISRM, Commission on Standardisation of Laboratory and Field Tests. Suggested methods for determining shear strength. Final Draft, 1974.

16. HUDSON, J.A. and BROWN, E.T. Studying the time-dependent effects in failed rock. In *Proc. Fourteenth Symposium on Rock Mechanics* edited by H.R. Hardy and R. Stefanko, American Society of Civil Engineers, New York, 1973, pp. 25–34.

17. ASTM. Standard Test Method for Triaxial Compressive Strength of Undrained Rock Core Specimens without Pore Pressure Measurements, D 2664-95a, 1995, pp. 1–4.

18. GAY, N.C. and JAGER, A.J. The influence of geological features on problems of rock mechanics in Witwatersrand mines. In: *Mineral Deposits of Southern Africa,* vols. I and II edited by C.R. Anhaeusser and S. Maske, Geological Society of South Africa, Johannesburg, 1986, pp. 753–772.

19. WAGNER, H. Protection of service excavations. In: Budavari, S. (Ed.). *Rock Mechanics in Mining Practice,* The South African Institute of Mining and Metallurgy. Monograph Series No. 5, Johannesburg 1983, pp. 201–220.

20. Chamber of Mines Research Organisation. An Industry Guide to Methods of Ameliorating the Hazards of Rockfalls and Rockbursts. Chamber of Mines of South Africa, Johannesburg, 1988, p. 70.

21. HANDLEY, M.F. Mining Strategies for the Ventersdorp Contact Reef at Depth. Regional Support Strategies at Depth. Papers and Discussions, The Association of Mine Managers of South Africa, May 1994–August 1996, pp. 183–201.

22. HANDLEY, M.F., HAGAN, T.O., and HOW, P.J. A borehole-dislocation sensor for the continuous monitoring of fracture displacement in deep mines. *J. S. Afr. Inst. Min. Metall.*, vol. 88, no. 2, February 1988, pp. 59–66. ◆